

Direct Identification of the Glass Transition: Growing Length Scale and the Onset of Plasticity

Einat Aharonov¹, Eran Bouchbinder², H. G. E. Hentschel³, Valery Ilyin², Nataliya Makedonska¹, Itamar Procaccia² and Nurith Schupper²

¹ *The Department of Environmental Sciences and Energy,*

² *The Department of Chemical Physics, The Weizmann Institute of Science, Rehovot 76100, Israel,*

³ *Dept. of Physics, Emory University, Atlanta, Georgia 30322.*

Understanding the mechanical properties of glasses remains elusive since the glass transition itself is not fully understood, even in well studied examples of glass formers in two dimensions. In this context we demonstrate here: (i) a direct evidence for a diverging length scale at the glass transition (ii) an identification of the glass transition with the disappearance of fluid-like regions and (iii) the appearance in the glass state of fluid-like regions when mechanical strain is applied. These fluid-like regions are associated with the onset of plasticity in the amorphous solid. The relaxation times which diverge upon the approach to the glass transition are related quantitatively.

Introduction: The understanding of the mechanical properties of amorphous solids cannot be dissociated from the elucidation of their structure, including the so-called glass transition which has eluded intensive research for quite some time. Plastic deformation, for example, arises from a qualitatively different physics in amorphous solids as compared to crystalline materials [1]. Since dislocation glide is precluded by the lack of crystalline order, much attention has been given to localized regions known as Shear Transformation Zones (STZ) [2, 3, 4, 5] which are believed to be loci of plastic responses to increased strain. In this Communication we demonstrate that a careful identification of liquid-like structures sheds unexpected light on the glass transition itself, including a sharp definition of the transition, an identification of the long-sought diverging length-scale [6] that accounts for the huge slowing down associated with the transition, and finally, a connection between the liquid-like defects and the onset of plastic deformations in the glass state.

The system: the glass former explored here is the well studied system of a two-dimensional binary mixture of discs interacting via a soft $1/r^{12}$ repulsion with a “diameter” ratio of 1.4. This two-dimensional model had been selected for simulation speed and, more importantly, for the ease of interpretation. We refer the reader to the extensive work done on this system [7], showing that it is a *bona fide* glass-forming liquid meeting all the criteria of a glass transition. In short, the system consists of an equimolar mixture of two types of particles with diameter $\sigma_2 = 1.4$ and $\sigma_1 = 1$, respectively, but with the same mass m . The three pairwise additive interactions are given by the purely repulsive soft-core potentials

$$u_{ab} = \epsilon \left(\frac{\sigma_{ab}}{r} \right)^{12}, \quad a, b = 1, 2, \quad (1)$$

where $\sigma_{aa} = \sigma_a$ and $\sigma_{ab} = (\sigma_a + \sigma_b)/2$. The cutoff radii of the interaction are set at $4.5\sigma_{ab}$. The units of mass, length, time and temperature are m , σ_1 , $\tau = \sigma_1\sqrt{m/\epsilon}$ and $T = \epsilon/k_B$, respectively, with k_B being Boltzman’s constant. A total of $N = 1024$ particles were enclosed in a square box (of area L^2) with periodic boundary con-

ditions, and our simulations followed verbatim those described in [7], giving us a most welcome check on the validity of our results. While Ref. [7] performed Molecular Dynamics, we ran both Molecular Dynamics and Monte Carlo simulations. The results shown below are in agreement between the two simulation methods. Ref. [7] found that for $T > 0.5$ the system is liquid and for lower temperatures dynamical relaxation slows down. A precise glass transition had not been identified in [7].

Analysis: to visualize the structural features of this system we employ the time-honored Voronoi polygon construction [8], where a polygon associated with any particle contains all points closest to that particle than to any other particle. The edges of such a polygon are the perpendicular bisectors of the vectors joining the central particle. As had been noted in [7, 8], the average coordination number is 6 at all temperatures, and local coordination numbers other than 6 are referred to as “defects”. Indeed, in previous work [7] the total concentration of “defects” was measured, see Fig. 1 upper panel, and it was concluded that although there is a slight decrease in this concentration when slowing down sets in, nothing dramatic is observed. We propose here that a more careful analysis is called for, in particular to distinguish between “fluid-like” defects and “glass-like” defects. We observe that only in the liquid phase there exist **small particles** enclosed in heptagons (or even octagons), and **large particles** enclosed in pentagons (or even squares) (cf. Fig. 2 upper panel). In the glass phase we observe only defects of the opposite type, i.e. small particles in pentagons and large particles in heptagons. We propose that the concentration of the liquid-like defects is a superior indicator of the glass transition in comparison with relaxation times. **The concentration c_ℓ of these liquid-like defects becomes so small in the glass phase that we cannot distinguish it from zero** (cf. Fig. 2 lower panel), unless the glass is put under mechanical strain, as shown below. Associated with this concentration we can define a typical scale, ξ , according to

$$\xi \equiv 1/\sqrt{c_\ell}. \quad (2)$$

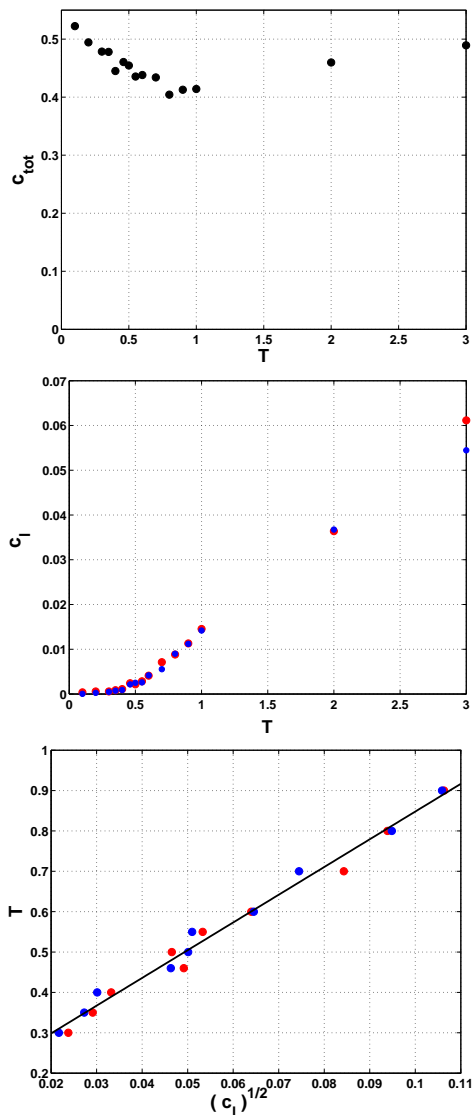


FIG. 1: Concentration of defects under slow cooling. Upper panel: the average concentration of all the defects as a function of temperature in black dots. Middle panel: the concentration of the liquid-like defects: large particles in pentagons (red dots) and small particles in heptagons (blue dots). Lower panel: the fit of the concentration of liquid-like defects as a function of temperature according to Eq. (4).

Associated with the strong decrease in c_ℓ we observe a huge increase in the typical scale ξ , in agreement with the tremendous slowing down of the dynamics.

In Fig. 1 middle panel we show c_ℓ as a function of the temperature for a protocol of slow cooling. For temperatures larger than 0.8 the concentration follows closely an exponential fit,

$$c_\ell = A \exp(-\Delta E/T), \quad A \approx 0.094, \quad \Delta E \approx 1.90. \quad (3)$$

For temperatures in the range $0.3 < T < 0.8$ we find an excellent fit to

$$c_\ell = B(T - T_g)^2, \quad B \approx 0.02, \quad T_g = 0.16 \pm 0.02. \quad (4)$$

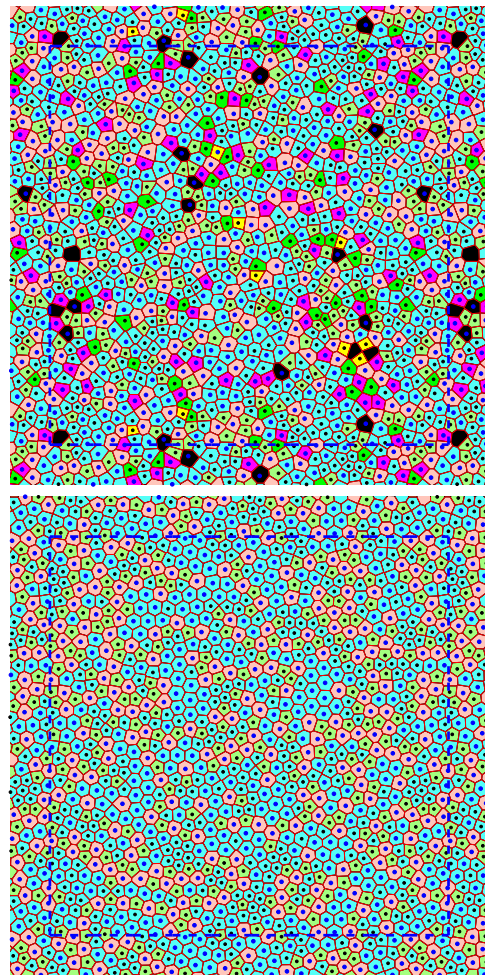


FIG. 2: Upper panel: The Voronoi polygon construction in the liquid state at $T = 3$ with the seven-color code used in this paper. Small particles in pentagons (heptagons) are light green (dark green) and large particles in pentagons (heptagons) are violet (pink). Lower panel: a typical Voronoi construction in the glass phase at $T = 0.1$. Note the total disappearance of liquid-like defects.

The quality of this fit is demonstrated in Fig. 1 lower panel. The fit (4) appears to identify a sharp glass transition $T_g = 0.16 \pm 0.02$; note, however, that there is no theoretical reason to expect that c_ℓ truly vanishes at T_g , but it becomes so small that we indeed do not see a single liquid-like defect in our finite-box simulations. We cannot exclude an exponentially small concentration that requires very much larger boxes to be observable. We can however state that T_g is finite since we demonstrate below that at temperatures lower than T_g the system reacts to shear like a solid. With the same range of temperatures we fit an apparently divergent length

$$\xi(T) \sim (T - T_g)^{-\nu}, \quad \nu = 1. \quad (5)$$

The same caveat applies: in fact we can only state that $\xi(T)$ becomes exponentially larger than the system size.

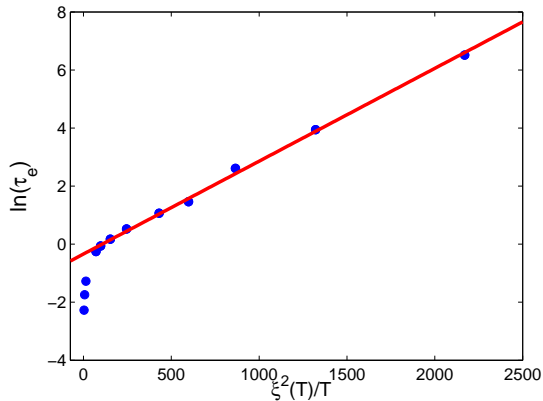


FIG. 3: The test of Eq. (7). The points are $\ln(\tau_e)$ as a function of $\xi^2(T)/T$. The solid line is a linear fit with $\tau_0 = 0.71$ and $\Delta\mu = 0.0055$.

At this point we connect this new structural definition of the glass transition to the more commonly considered criterion, i.e. the relaxation time (or viscosity), and show the one-to-one correspondence between the two. The relaxation times τ_e for the same system were measured in [9] via the decorrelation times of the scattering functions, as a function of T , for $0.4 < T < 5$. To connect between the relaxation time τ_e and the length scale ξ we assume as usual [10] that for the viscous fluid there exists a free energy of activation $\Delta G^*(T)$ associated with the relaxation event,

$$\tau_e = \tau_0 \exp(\Delta G^*(T)/T), \quad (6)$$

where τ_0 is a microscopic time scale of the order of a single particle vibration time. The free energy of activation is estimated as the number of Voronoi cells $N^*(T)$ involved in the relaxation event, times the (temperature independent) chemical potential per cell $\Delta\mu$, $\Delta G^*(T) \approx N^*(T)\Delta\mu$. The number N^* is now taken as the typical number of Voronoi cells in regions that are free of liquid like defects, and therefore $N^*(T) \approx \pi\xi^2(T)/4\bar{\Omega}$, where $\bar{\Omega}$ is the mean area of a Voronoi cell. We thus end up with the prediction

$$\tau_e = \tau_0 \exp(\pi\xi^2(T)\Delta\mu/4\bar{\Omega}T). \quad (7)$$

Using now $\xi \approx 1/\sqrt{c_\ell}$ together with the fits (3) and (4) we can compare the prediction (7) to the measured relaxation times given in [9]. This comparison is presented in Fig. 3, where we see an excellent agreement with $\tau_0 = 0.71$ and $\Delta\mu = 0.0055$. This value of τ_0 is of the order of the expected particle vibration time [7]. At the highest values of the temperature, $T > 2$, the concentration of liquid-like defects is too high, and the law (7) does not apply.

Note that in our calculation we did not follow the traditional steps of Adam and Gibbs who, due to the lack of independent knowledge of N^* , assume that $N^*/s_c^* = N/S_c$

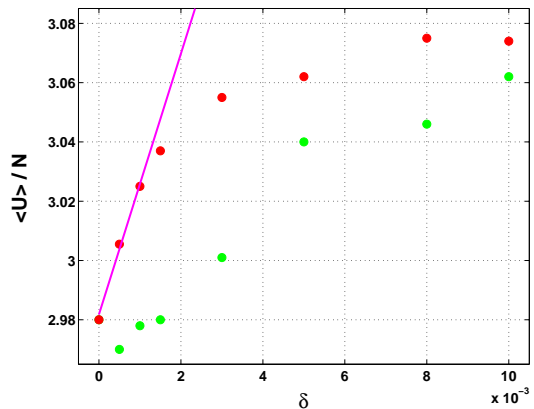


FIG. 4: The response of the system to shear. The measured energy of the system after the shear is applied is shown in red dots. The rhombic box is then returned to a square box and the energy at the end is shown in green dots. For small values of δ the energy grows linearly in δ . When the value of δ exceeds 10^{-3} the linear dependence is lost, apparently due to a plastic response, and upon the return to the square box memory is not lost and the energy does not return to the initial value.

where s_c^* is the configurational entropy of the region involved in the relaxation, whereas S_c is the total configurational entropy of the system. In our view this step is questionable, since it appears that the configurational entropy per particle of the whole system, including the liquid-like defects, is higher than the constrained configurational entropy per particle of the region which is free of liquid-like defects. Indeed, we predict that the relaxation time diverges where $c_\ell \rightarrow 0$, (i.e. at T_g) whereas the Adam-Gibbs formula predicts divergence only when $S_c \rightarrow 0$ (i.e. at the Kauzmann temperature T_k if the latter exists [11]). We thus conclude that the two definitions of a glass transitions appear to agree on the existence of a finite value T_g where the fluid becomes a glass. We stress that it is considerably easier to determine $\xi(T)$ at low temperatures than to measure $\tau_e(T)$. The latter quantity becomes inaccessible to measurement due to jamming. The concentration of liquid-like defects is much easier to determine since the Voronoi tessellation remains highly mobile even in the glass phase. Minute changes in particle positions is reflected in changes in the Voronoi cells, allowing statistics to be accumulated at temperatures where the usual relaxation measurements become quite impossible. For this reason we are in a much better position to fit a finite value of T_g .

The onset of plasticity: having identified the glass transition with the disappearance of liquid-like defects, we proceed to strengthen this identification by analyzing the response of the glass state to a mechanical strain. In particular we show that for $T < T_g$ the system exhibits a finite shear modulus as is expected from a solid. To this aim we applied strain on the system in the glass phase, always starting from conditions as in Fig. 2 lower panel. The square box was strained to a rhombic form keeping

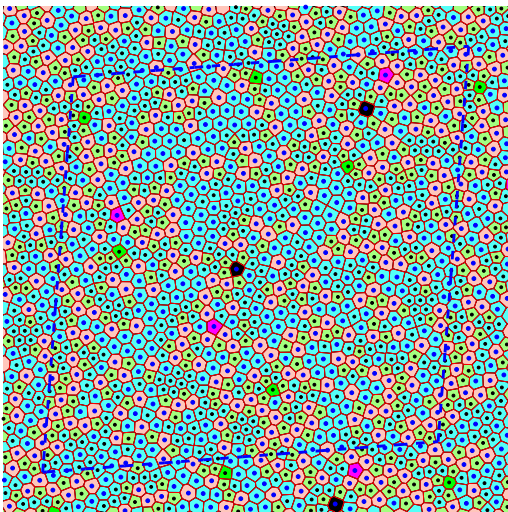


FIG. 5: A strained configuration after the linear elastic response is lost, $\delta = 3 \times 10^{-3}$. Notice the reappearance of liquid-like defects.

the area constant. This linear straining transformation is determined by the matrix \mathbf{h} ,

$$\mathbf{h} \equiv \mathbf{1} + \boldsymbol{\epsilon} = \begin{pmatrix} 1 + \delta & \sqrt{(1 + \delta)^2 - 1} \\ \sqrt{(1 + \delta)^2 - 1} & 1 + \delta \end{pmatrix}, \quad (8)$$

where $\boldsymbol{\epsilon}$ is the strain tensor. The linear elastic energy density associated with such a transformation is

$$\frac{U_{\text{el}}}{L^2} = \frac{1}{2} \lambda \epsilon_{kk}^2 + \mu \epsilon_{ij} \epsilon_{ij} = (2\lambda + 4\mu) \delta^2 + 4\mu \delta, \quad (9)$$

where λ and μ are the 2-dimensional Lamé coefficients. In all our simulations we applied the transformation with a chosen value of δ , allowed the system to relax by Monte Carlo steps in the strained configuration, and then we applied the inverse transformation, returning to the square box. The results of these simulations are most revealing. For small values of δ , $\delta < 10^{-3}$, the system responds elastically, see Fig. 4. In this regime the energy increases linearly with δ as expected from the leading term in Eq.

(9). As long as the response is elastic, it is also reversible: upon returning to the square box the energy returns back to its initial value. On the other hand, when the value of δ exceeds 10^{-3} the linear dependence is lost, but *not according to the elastic prediction Eq. (9)*. Rather than curving up as a function of δ , the energy is curving down, apparently due to a plastic response; Indeed, upon the return to the square box memory is not lost and the energy does not return to the initial value. **Most interestingly, for values of strain where the linear elastic response is lost, the strained configuration exhibits a significant concentration of liquid-like defects**, see Fig. 5. We propose that these liquid-like defects are the STZ that are the loci of plastic responses. Quite characteristically, once these appear, the mechanical response is not reversible, as seen in Fig. 4. There is a remnant stress now, exhibiting the well known hysteretic behavior associated with the onset of plasticity.

Summary: in summary, we have presented a novel view of the glass transition, identifying the transition as associated with the disappearance of liquid-like defects. A diverging correlation length was identified and measured. We demonstrated that this divergence coincides with the divergence of the relaxation time as measured from standard time-correlation functions. The very same local arrangements of particles which is identified as liquid-like defects reappears once again when plasticity sets in under strain. In a subsequent publication we will present the statistical mechanics of this phenomenology, explaining and substantiating further the findings presented here.

Acknowledgments

IP thanks Peter Harrowell for showing him the beauty of this subject. We benefitted from discussions and exchange of ideas with Michael Falk and Jim Langer. This work had been supported in part by the Israel Science Foundation, by the Minerva Foundation and by the German-Israeli Foundation. EB is supported by the Horowitz Center for Complexity Science.

-
- [1] I. Kovács and L. Zsoldos, *Dislocations and Plastic Deformation* (Pergamon press, Oxford 1973).
- [2] A.S. Argon, *Acta Metall. Mater.* **27**, 47 (1979).
- [3] M.L. Falk and J.S. Langer, *Phys. Rev. E* **57**, 7192 (1998).
- [4] E. Bouchbinder, J. S. Langer and I. Procaccia, "Athermal Shear-Transformation-Zone Theory of Amorphous Plastic Deformation I: Basic Principles", submitted to *Phys. Rev. E*. Also: cond-mat/0611025.
- [5] E. Bouchbinder, J. S. Langer and I. Procaccia, "Athermal Shear-Transformation-Zone Theory of Amorphous Plastic Deformation II: Analysis of Simulated Amorphous Silicon", submitted to *Phys. Rev. E*. Also: cond-mat/0611026.
- [6] L. Berthier, G. Biroli, J.-P. Bouchaud, L. Cipelletti, D. El Masri, D. L'hôte, F. Ladueu and M. Pierno, *Science* **310**, 1797 (2005).
- [7] D.N. Perera and P. Harrowell, *Phys. Rev. E* **59**, 5721 (1999) and references therein.
- [8] D. Deng, A.S. Argon and S. Yip, *Philos. Trans. R. Soc. London Ser A* **329**, 549, 575,595, 613 (1989).
- [9] D. N. Perera and P. Harrowell, *J. Chem. Phys.*, **111**, 5441 (1999).
- [10] G. Adam and J.H. Gibbs, *J. Chem. Phys.* **43**, 139 (1965)
- [11] W. Kauzmann, *Chem. Rev.* **43** 219 (1948).